J. Indian Inst. Sci., May–June 1995, 75, 321–331
© Indian Institute of Science

Ultra-fast solvation and electron transfer dynamics in dipolar liquids

BIMAN BAGCHI
Solid State and Structural Chemistry Unit, Indian Institute of Science, Bangalore 560 012 and Jawaharlal Nehru Centre of Advanced Scientific Research, Jakkur, Bangalore 560 064, India.

Abstract

A recently developed microscopic theory of ultra-fast solvation dynamics of an ion in dipolar liquid is briefly reviewed. The theory has been applied to explain observed solvation dynamics in liquid water and acetonitrile. For both these liquids, the calculated solvation time correlation function shows an ultra-fast Gaussian decay which is followed by an exponential-like, much slower, decay. The interesting fact is that the initial Gaussian decay dominates the relaxation to the extent that it contributes about 60–80% to the total decay. These results are in excellent agreement with all the available computer simulation and experimental results. We find that both the rotational and the translational librational modes of water contribute significantly to the initial Gaussian decay. Since electron transfer reactions are often controlled by the solvation (as in the Marcus theory), we have carried out a detailed analysis of the dynamic effects of the ultra-fast solvation on electron transfer reactions in the above liquids. It is found that the ultra-fast solvation can have novel effects on the rates of electron-transfer reactions in these liquids.

Keywords: Ultra-fast solvation dynamics, electron-transfer dynamics, ion, dipolar liquid, electrical perturbations,

1. Introduction

The dynamics of solvation of a newly created ion in dipolar liquids is a subject of tremendous current interest in physical chemistry. Recently an international effort has been directed to understand this problem[1–18]. This effort has led to some spectacular discoveries and, as a whole, led to a much better understanding of the dynamics of complex dipolar liquids which are so relevant as solvents in many chemical, biological and industrial processes.

In this article a general molecular theory of solvation dynamics developed by us shall be discussed with applications to two common dipolar liquids, namely, water and acetonitrile. Both these liquids are known to be rather fast in their response to electrical perturbations. Initial experimental work was done by Barbara and coworkers[2]. Solvation in water was found to be biexponential with time constants approximately equal to 250 fs and 1.2 ps. This study could not resolve the initial part of solvation dynamics. Computer simulations provided a more detailed, but somewhat different, information. The important work of Maroncelli and Fleming[3,19] revealed three notable features. First, the solvation is dominated by a Gaussian component which decays within a few tens of femtoseconds and

*Text of invited talk delivered at the Annual Meeting of the Faculty of the Jawaharlal Nehru Centre for Advanced Scientific Research at Bangalore on November 11, 1994.

which carries about 70–90% of the solvation energy. This is followed by a marked oscillation in the solvation time correlation function. The last phase of the decay is slow and exponential-like with time constant of the order of a 1 ps or so. The situation was similar in acetonitrile where initial experimental studies revealed only the exponential-like decay while the simulations of Maroncelli[20] suggested a significant contribution from the ultra-fast Gaussian component. This paradoxical situation was resolved with the landmark experiment of Rosenthal *et al.*[21] who measured solvation dynamics in acetonitrile with a much better time resolution than hitherto possible. This experimental study of solvation in acetonitrile established beyond doubt the importance of the initial, Gaussian component in ultra-fast solvation. The long time decay was exponential-like, like the one observed experimentally[3]. Recently, Jimnez *et al.*[11] presented the experimental result of ultra-fast solvation in water. The features of solvation were similar to those obtained for acetonitrile and also from simulations. The notable differences from simulations were somewhat slower decay of the ultra-fast component (54 fs instead of 15–20 fs) and the oscillations were absent. Theoretical studies discussed here in are in striking agreement with the observed results. Similar results have been observed even for simple model liquids like a Stockmayer liquid[22]. Thus, we may regard the biphasic solvation in fast liquids fully established.

However, there is still need to understand the reason for the great separation of time scales between the initial Gaussian decay and the subsequent slow, exponential-like decay. It has been suggested[23–26] that the Gaussian decay is due to the librational modes of water while the long time decay is due to the diffusive dynamics involving primarily the nearest-neighbour molecule. This interpretation raises several questions. First, why is the relative contribution of the Gaussian component so large when the librational modes themselves contribute only a small amount to the total dielectric relaxation? Second, can we explain *quantitatively* the slow long time decay? Its description in terms of the nearest-neighbour molecules is somewhat vague. And lastly, what is the role of the intermolecular vibrational modes that are well known in liquid water[27]?

The microscopic treatment presented here provides answers to many of the above questions, in addition to providing a unified theoretical description. The calculated solvation dynamics has a rich structure and is in agreement both with computer simulations[19, 20, 22] and experiments[11, 21]. What is perhaps more important is the interpretation of the various stages of solvation that this study provided and this is articulated below. In particular, we find that both the rotational *and the intermolecular vibrational* modes contribute significantly to the initial relaxation of the solvation energy. Another significant result is that the neglect of molecular polarizability might have led to a faster solvation in classical simulations than would occur in real water.

There are two major ingredients of all the existing theories of solvation dynamics. First, one requires a description of the static equilibrium orientational correlations. One requires both the ion–solvent and solvent–solvent pair correlation functions. Fortunately, these correlations are now becoming increasingly available for real dipolar liquids[28]. The second important ingredient is the wave vector and frequency-dependent dissipative kernel which is a measure of the dynamic response of the polar liquid. We require both the rotational and the translational dissipative kernel, although the former is clearly more im-

portant for ultra-fast dynamics. It is prohibitively difficult to calculate these quantities. The only alternative, therefore, is to obtain them directly from experiment. However, this also requires an accurate microscopic expression relating an experimental observable with the dissipative kernel. This expression is inevitably an expression for a time correlation function which can be inverted to obtain the dissipative kernel in terms of the correlation function. The problem with this scheme is that the observables that are readily available contain only in the long wavelength (or zero wavenumber) information. Therefore, we can obtain by this method only the long wavelength, although full frequency-dependent, dissipative kernel.

Another problem addressed to in this paper is the effects of this newly discovered ultra-fast solvation on the rates of adiabatic electron-transfer reactions. One expects these effects to be significant because in electron-transfer reaction, it is the solvation energy that is the reaction coordinate[29–33]. Recent theoretical studies have indicated that the ultra-fast solvation can indeed have large effects on the nature of electron transfer in water, acetonitrile and methanol[33–38].

The organization of the rest of the paper is as follows. In the next section we present the theoretical formulation. In Section 3, we present the numerical results. In Section 4 we present the results of our work on electron-transfer reaction. Section 5 concludes with a brief discussion.

2. Theoretical formulation

The theoretical formulation is next briefly described. The time-dependent solvation energy is given by the following expression[1, 23]

$$E_{sol}(t) = -\frac{1}{2.(2\pi)^3}\int dk\; E_0(-k).P(k,t), \tag{1}$$

where $E_0(k)$ is the Fourier-transformed bare electric field of the ion with k as the Fourier variable conjugate to the position variable r. The wave-vector and time-dependent solvent polarization $P(k,t)$ is defined by

$$P(k,t) = \int d\Omega\; \mu(\Omega)\rho(k,\Omega,t), \tag{2}$$

where $\mu(\Omega)$ is the dipole moment vector with orientation Ω and $\rho(k, \Omega, t)$ is the wave-vector, orientation (Ω) and time-dependent number density of the solvent molecules. Next, $\rho(k, \Omega, t)$ is expanded in spherical harmonics as

$$\rho(k,\Omega,t) = \sum_{l,m} a_{lm}(k,t)\, Y_{lm}(\Omega). \tag{3}$$

The solvation dynamics of an ion probe $a_{10}(k,t)$ which is related to longitudinal polarization by[1,5,23]

$$P_L(k,t) \equiv P(k,t).k = \frac{4\pi}{3}\mu\, a_{10}(k,t). \tag{4}$$

The molecular hydrodynamic approach, described elsewhere[23], provides the following general expression for $a_{1m}(k, z)$

$$a_{10}(k,z) = \frac{a_{10}(k,t=0)}{z+\sum_{10}(k,z)}, \tag{5}$$

where the generalized rate $a_{10}(k, z)$ as given by[23]

$$\Sigma_{10}(k,z) = \frac{1(1+1)\, f_{110}(k)}{z+\Gamma_R(k,z)} + \frac{p k^2 f_{110}(k)}{z+\Gamma_T(k,z)}, \tag{6}$$

Here, $a_{10}(k, z)$ is the Laplace transform of $a_{10}(k,t)$ with z as the Laplace frequency, scaled in the units of $\iota_I = (\beta I)^{1/2}$ with β as the inverse of temperature in the energy units. $f_{110}(k) = 1 - (\rho_0/4\pi)\, c_{110}(k)$ is the 'caging parameter' where $c_{110}(k)$ is the (110) component of the spherical harmonic expansion of the two-particle direct correlation function in the intermolecular frame. For a solvent molecule of mass M, diameter σ and moment of inertia I, the translational parameter, $p = I/M\sigma^2$ measures the relative importance of the solvent translational modes in comparison to the rotational ones. $\Gamma_R(k, z)$ and $\Gamma_T(k, z)$ are the dissipative kernels for rotational and translational motions of the solvent molecules. The final expression for the time-dependent solvation energy of an ion of charge Q is given, in the frequency space, by the following rather elegant expression[23].

$$E_{sol}(z) = -\frac{Q^2}{\pi\sigma}\int dk \left(\frac{\sin k}{k}\right)^2 k^2 \left[1-\frac{1}{\varepsilon_L(k)}\right] \frac{1}{z+\sum(k,z)} \tag{7}$$

where $\varepsilon_L(k)$ is the longitudinal component of the wave-vector-dependent dielectric relaxation, related to $f_{110}(k)$[8,9]. The time-dependent solvation energy can be obtained from eqn 7 by Laplace inversion.

The two quantities of crucial importance in the expression for solvation energy are the 'caging parameter', $f_{110}(k)$ and the dissipative kernels, $\Gamma_X(k,z)$, $X=R,T$. $f_{110}(k)$ has a strong dependence on the wave-vector k. It is large and positive near $k = 0$ as it is approximately proportional to the static dielectric constant, E_0. But it undergoes a dramatic decrease in value near $k \simeq 2\pi/s$, which corresponds to the nearest neighbour distance. This decrease in $f_{110}(k)$ implies, in turn, a pronounced slowing down of the relaxation of $a_{10}(k, t)$. In the present work, we have used $f_{110}(k)$ which has been calculated recently by Rainari *et al.*[28] for liquid water. It must, however, be emphasized at this juncture that the k-dependence of $f_{110}(k)$ and hence of $\varepsilon_L(k)$, *is nearly universal*, as can be seen if we plot these functions, as obtained by different model calculations, including MSA and ISM or computer simulations. This makes the present calculation of solvation dynamics nearly model free.

As discussed in the Introduction, the determination of the dissipative kernel is highly non-trivial and forms the bottleneck in any microscopic study of orientational relaxation in dense dipolar liquids. And, it is especially complicated for liquid water which shows a complex dynamics. In this work, we shall neglect the wave-vector dependence of the dissipative kernels. This is justified in the short time when essentially the static correlations

determine momentum and angular momentum dissipations. We have shown elsewhere[23,24] that this assumption is valid for the ultra-fast solvation in the model Stockmayer liquid[22], where $\Gamma_R(k=0, z) = \Gamma_R(k \to 0, z)$ with surprising accuracy. We next describe how to obtain $\Gamma_R(k=0, z)$ from the dielectric relaxation and the far-infrared (FIR) spectrum of liquid water. First note that the frequency-dependent dielectric function, $\varepsilon(z)$ [$= \varepsilon(k=0, z)$] is related to $a_{10}(k=0, z)$ by the following linear response expression

$$1-\frac{1}{\varepsilon(z)}=\frac{4\pi\beta}{V}\left[C_{ML}(k=0,t=0)-z\,C_{ML}(k=0,z)\right], \tag{8}$$

where $\beta=(k_BT)^{-1}$, k_B, the Boltzmann constant, T, the absolute temperature, and V, the total volume of the system. $C_{ML}(k, z) = (4n/3)\mu^2 < a_{10}(k, t=0)\ a_{10}(k, z) >$ is the longitudinal component of the total moment autocorrelation function. Therefore, eqns 5 and 6 can be inverted to obtain $\Gamma_R(z)$ in terms of the frequency-dependent dielectric function $\varepsilon(z)$, as given by the following elegant expression[23]

$$\frac{1}{z+\Gamma_{10}(z)}=\frac{z}{2f_{110}(k=0)}\cdot\frac{\varepsilon_0[\varepsilon(z)-n^2]}{n^2[\varepsilon_0-\varepsilon(z)]}, \tag{9}$$

where n is the refractive index of liquid water. The details of the derivation of eqn 9 are available elsewhere[23].

The frequency-dependent dielectric function derives contributions both from the Debye dispersion and the librational modes of the water molecules. The expression for $\varepsilon(z)$ is then given by[23-26]

$$\varepsilon(z)=n^2+\frac{\varepsilon_0-\varepsilon_\infty}{1+z\tau_D}+(\varepsilon_\infty-n^2)(1-z\,\phi_{lib}(z)), \tag{10}$$

where the Debye relaxation time, $\tau_D = 9.33$ ps, and the infinite frequency dielectric constant, $\varepsilon_\infty = 4.86$, are obtained by fitting to Debye formula[40]. For water, n is equal to 1.33. $\phi_{lib}(z)$ is the librational moment correlation function. This is calculated from the model of a damped harmonic oscillator with the experimental librational frequency equal to 199 cm^{-1} and a damping factor of 100 cm^{-1}.

We next describe the calculation of the translational dissipative kernel. This can certainly be obtained from dynamic structure factor. However, there is a simpler and more convenient procedure, which is described below. First note that the translational contribution is important only at intermediate to large k. In this domain, the dissipative kernel is given accurately by its single particle limit and the following memory function relation between the Laplace transform of the velocity correlation function and the dissipative kernel holds

$$C_v(z)=\frac{C_v(t=0)}{z+\Gamma_T(z)}. \tag{11}$$

In their important work, Rahman and Stillinger[41] provided accurate $C_V(z)$. It has two librational peaks at frequencies near 44 cm^{-1} and 215 cm^{-1}. We have fitted $C_V(z)$ to the fig-

ure provided by these authors. We have now all the ingredients to determine $E_{sol}(z)$ completely. We obtained $E_{sol}(t)$ by numerically Laplace inverting $E_{sol}(z)$.

We have checked the accuracy of our method of obtaining the dissipative kernel. The idea is that if the k-dependence is really weak, then the rotational diffusion constant, D_R, calculated from the Einstein relation $D_R = (\beta I \Gamma_R(k=0, z=0)^{-1}$ (with $I_R(k=0, z=0)$ given by eqns 9 and 10), should be in good agreement with the known D_R. We find a value of $D_R = 2.2 \times 10^{11}$ s^{-1}. Two different computer simulations give values equal to 3.6×10^{11} s^{-1} and 1.6×10^{11} s^{-1} [42]. Thus, the agreement is quite good. An experimental measure of this self-diffusion coefficient can be obtained from the Debye relaxation time, τ_D itself by using the following macro–micro relation[8] between $(2D_R)$ and τ_D[5]

$$\tau_D = (2D_R)^{-1}[1 + (\rho_0 / 4\pi) c_{111}(k=0)]. \tag{12}$$

This provides a value equal to 2.2×10^{11} s^{-1} which is perfect. All these evidences lead us to conclude that the assumption of the weak k-dependence of the rotational dissipative kernel is valid for liquid water. We next present the results of our numerical calculations.

For acetonotrile, the most accurate information of the ultra-fast solvent response is obtained from Kerr relaxation studies of MacMorrow and Lotshaw[43]. In the study reported below, the Kerr relaxation data has been used to obtain the rotational memory function which is then used to obtain the solvation time correlation function.

3. Numerical results on solvation dynamics

We calculate the solvation time correlation function, $S(t)$, defined as[1–6]

$$S(t) = \frac{E_{sol}(t) - E_{sol}(\infty)}{E_{sol}(0) - E_{sol}(\infty)}. \tag{13}$$

The calculated $S(t)$ for water and acetonitrile are shown in Figs 1 and 2. In both the cases, we have compared our theory with the experimental results. First note that the agreement is excellent in both the cases. While in the case of water, no adjustable or free parameter was used, in the case of water we need to make the 199 cm^{-1} intermolecular vibrational band overdamped to remove the oscillation at the intermediate time. Second, the solvation time correlation function in both the cases exhibits a pronounced biphasic character. The initial decay is extremely rapid and Gaussian in time. For water, this ultra-fast component accounts for the completion of 50–60% of solvation in less than 50 fs. After the oscillation, the rest of the decay is slow and exponential-like, but not single exponential. This part of the decay can be fitted to a sum of two exponentials, with time constants of 250 fs and 1 ps. This agrees quite well with the observation of Barbara and Jarzeba[2]. For acetonitrile, the ultra-fast component carries even larger contribution (70–80%) but the time constant is somewhat larger, about 100 fs. The difference between the two liquids can be understood by considering relative contributions and the relevant time constants of the librational and the orientational motions. Water, because of its extended hydrogen bond network, contains significant amount of librational and vibrational motions which are almost absent in acetonitrile. The latter, however, has very fast, partly inertial (because of its nearly spherical shape), single particle reorientational motion

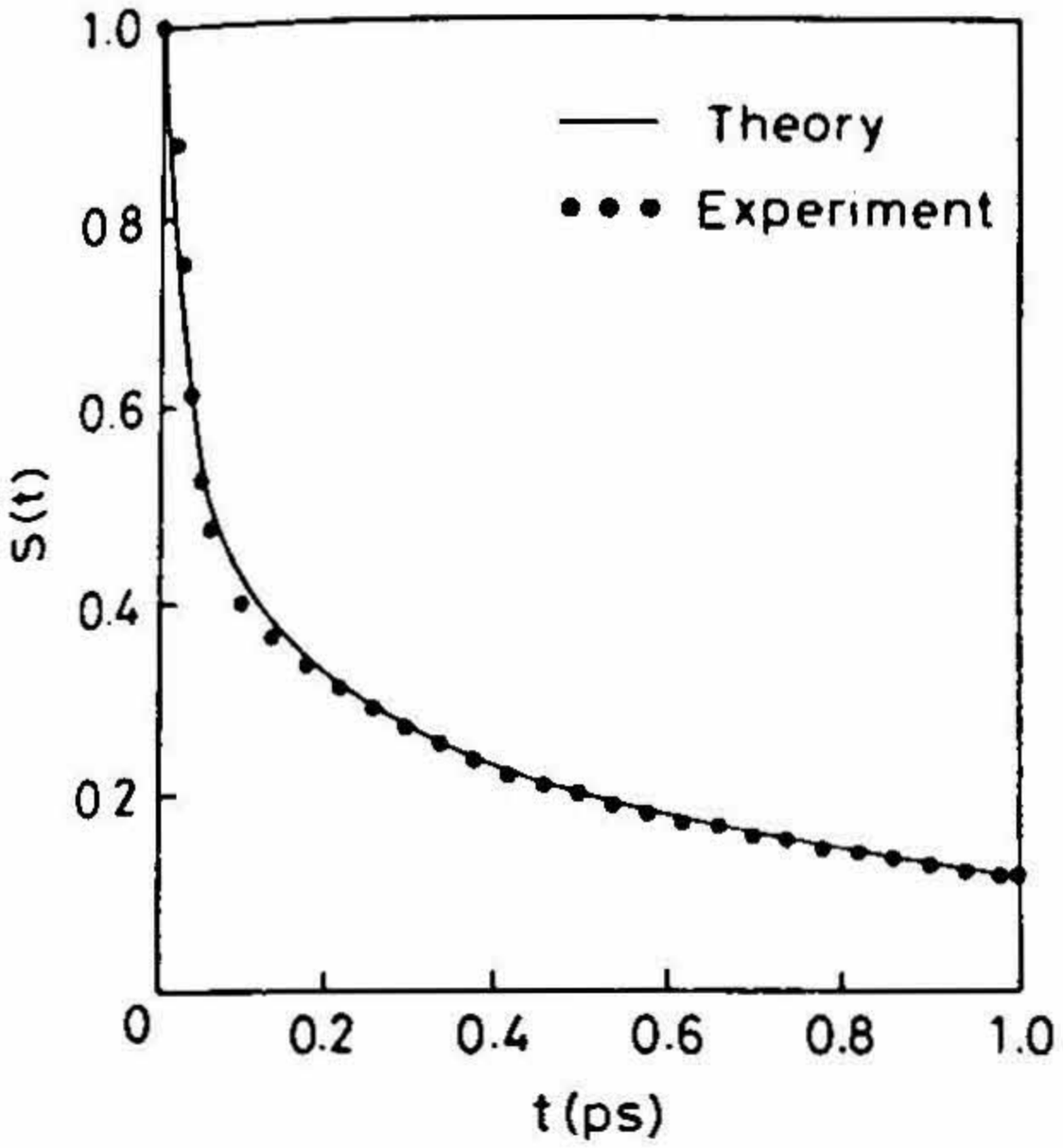

FIG. 1. The comparison between theoretical prediction and experimental results on solvation dynamics in water. The solid line is the theoretical prediction (eqn 7) while the solid dots are the experimental results of Jimnez *et al.*[11]. The theory has no adjustable parameter[25].

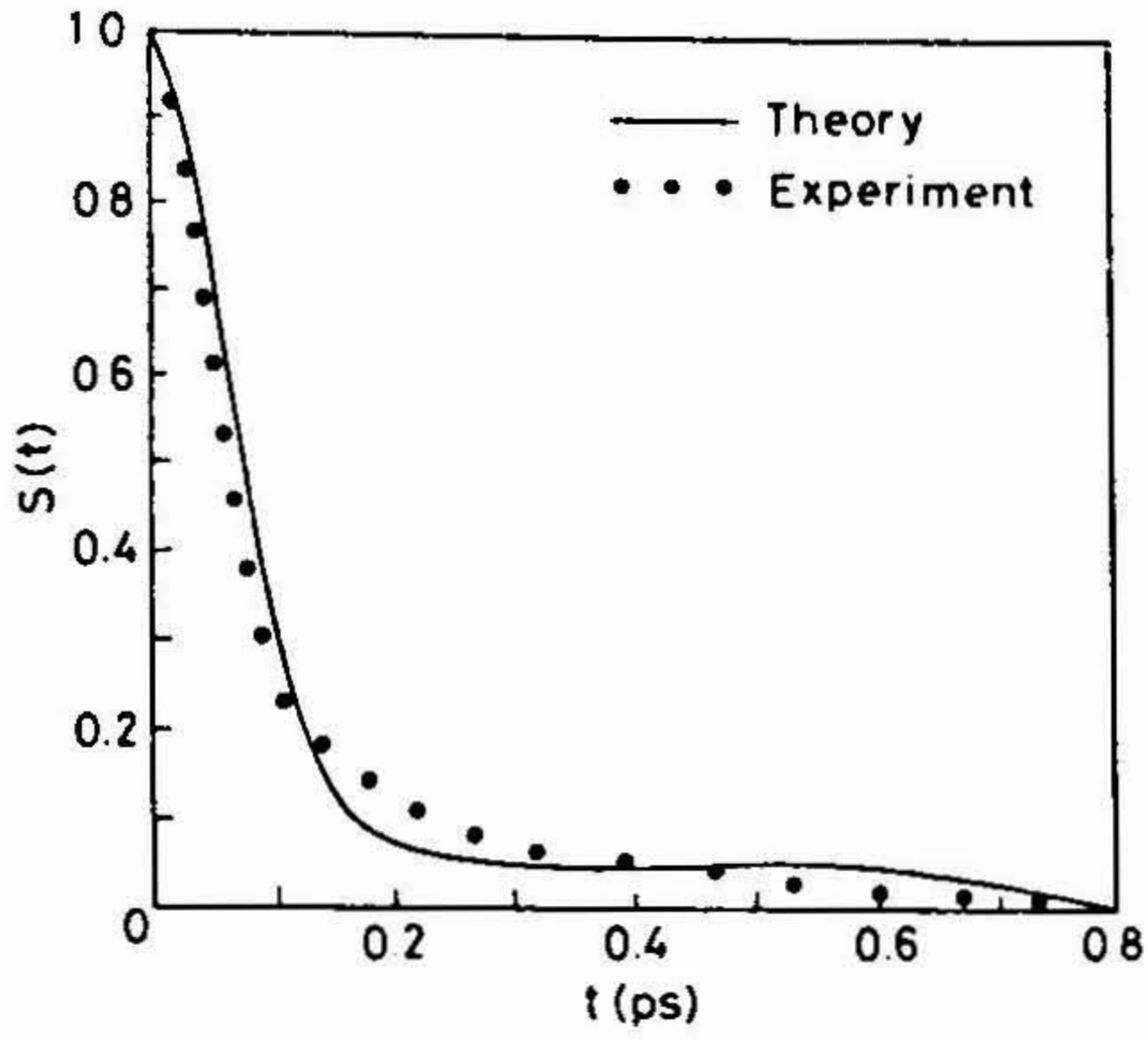

FIG. 2. The comparison between theoretical prediction and experimental results on solvation dynamics in acetonitrile. The solid line is the theoretical prediction (eqn 7) while the solid dots are the experimental results of Rosenthal *et al*[21]. The theory has no adjustable parameter[24].

which responds in the ultra-fast time scale. Another key aspect, often ignored, is the high polarity of the solvent that is essential in setting the frequency of the solvation energy surface. The rate of solvent is determined jointly by the frequency of the driving force and the linear response of the solvent.

4. Electron-transfer reactions

Since the important work of Zusman[30] on the solvent effects in outersphere electron transfer reactions, considerable effort was directed to understand these effects in more detail[31–34]. Experimental results reveal dramatically different solvent dependencies which range from virtually no role of solvent relaxation to the cases where such relaxation is rate determining. Recently, we investigated the effects of ultra-fast solvation in water and acetonitrile, discussed above, on the rates of adiabatic electron-transfer reactions in these solvents[35–38]. In the following we summarize the main results.

The reaction studied was the electron transfer in the following model system[31]

$$OX + e \rightarrow \text{Red.}$$

In the one-dimensional Marcus model, the reaction coordinate is the fluctuating energy gap, $\Delta E(t)$, between the two equilibrium surfaces. For this reaction, the reaction coordinate becomes the solvation energy of a charge e. It is further assumed that the acceptor and the donor are in contact and that they are spheres of the same size. In order

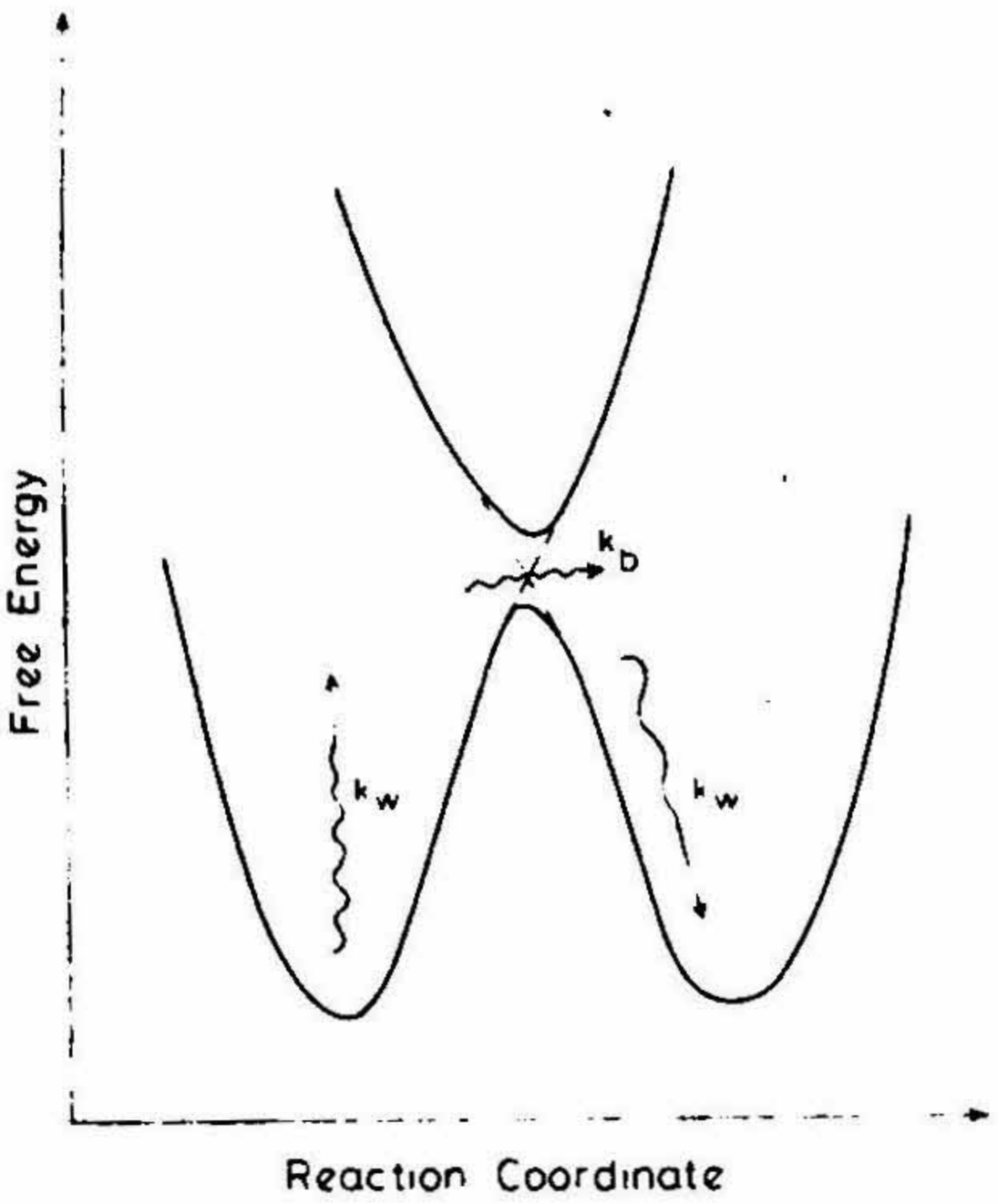

FIG. 3. A schematic illustration of the reaction potential energy diagram usually employed in the study of electron-transfer reaction (ETR). The situation shown here corresponds to a weakly adiabatic electron-transfer reaction which is formed from two diabatic surfaces which are shown by dashed lines. In the given example, the rate of ETR is determined by the twin rates of well-relaxation (k_w) and barrier crossing (k_b). These rates are also indicated in the figure.

to calculate the rate of an outersphere adiabatic electron-transfer reaction in an ultra-fast solvent, we need to calculate both the rate of energy diffusion required to reach the barrier top (k_{ed}) and the rate of barrier crossing (k_b). The reaction potential energy surface is shown in Fig. 3. The total rate of electron transfer is given by the following expression

$$(k_{et})^{-1} = (k_{ed})^{-1} + (k_b)^{-1}.$$

Both k_{ed} and k_b are determined, in addition to the reaction potential energy parameters, and the reaction time correlation function, $c_{EE}(t) = \langle E(0)\ E(t) \rangle$. Now, the connection with the solvation dynamics comes from the equivalence between $S(t)$ and $C_{EE}(t)$. This is, in essence, the assumption of linear response and seems to be generally valid for solvation of ions.

In theoretical calculations, the adiabaticity of a reaction is often expressed in terms of the ratio of the barrier frequency (ω_b) to the reactant well frequency (ω_0). This ratio is of the order of unity for an adiabatic reaction while it can be much larger one for a weakly adiabatic reaction. The terms involved in the calculation of the barrier crossing rates are the Grote–Hynes reactive frequency λ_R and the transmission coefficient κ. The rate of barrier crossing is given by $k_b = \kappa k^{TST}$, where k^{TST} is the barrier crossing rate. As the ratio ω_b/ω_0 increases, one expects the transmission coefficient to approach unity as dynamic solvent effects become less important when this ratio is very large. The method to calculate the energy diffusion is entirely different. Here we calculate the mean first passage time to reach the barrier top starting from the zero point energy in the reactant

Table I
Calculated rates of barrier crossing

Solvent	ω_b/ω_0	λ_R	κ	ν_b
Acetonitrile	0.5	1.1193	0.3658	0.3563
	1.0	4.4834	0.7326	0.7136
	1.8	11.0149	0.9998	0.9739
Water	1.0	1.1603	0.2397	0.1847
	5.0	20.3395	0.8405	0.6474
	9.0	43.0134	0.9875	0.7606

[$\kappa = (\lambda_r/\omega_b) = (\kappa_b/\kappa^{TST})$; $\nu_b = \nu_b^{TST}$ κ = frequency of barrier crossing from Grote–Hynes theory; $\nu_b^{TST} = \omega_0/2\pi$.]

well. Here the barrier frequency is not involved, as we have approximated the reactant well by a harmonic well with frequency; ω_0. Here the important dynamical quantity is the net frequency of electron transfer which is given by $\upsilon_{ed} = k_{ed} \exp(\beta E_a)$, where E_a is the Marcus activation energy.

In Tables I and II we show the calculated values of the rates of electron transfer along with the individual rates of barrier crossing and energy diffusion[36–38]. Note that in Table I the predicted transition state rate (ν_b) should be unity in the scaled unit. Table II shows the surprising prediction that for acetonitrile, the rate can be in the energy diffusion-controlled regime while for water it is still dominated by the barrier crossing. In fact, the predicted rate of electron transfer is close to the transition state rate for water. In acetonitrile, however, the rate falls below the TST rate because of slow rate of energy diffusion. Thus, the latter provides an extreme example of energy diffusion limited rate. These predictions can be verified experimentally.

5. Conclusion

In the present work, the slow long time decay observed both for water and acetonitrile originates from the strong orientational correlations present at the molecular length scales, where $c_{110}(k)$ reaches a maximum and consequently $f_{110}(k)$, a minimum[1,5]. This produces a considerable slowing down in the rate of energy relaxation. Translational modes of the solvent molecules are important in this regime. The initial Gaussian decay arises primarily from the librational modes (especially for water) and the fast orientational motions. *What makes it so dominant is the large value of* $f_{110}(k=0)$ *which is equal to* 11.71 *for liquid water.*

Table II
Calculated rates of energy diffusion and the rates of electron transfer

Solvent	ω_0	βE_a	υ_{ed}	ν_b^{TST}	υ_{et}
Acetonotrile	6.12	9.88	0.1295	0.5618	0.1052
Water	4.84	27.1	124.88	0.7703	0.7656

[$\upsilon_{ed} = k_{ed} \exp(\beta E_a)$ frequency of energy diffusion, $\upsilon_{et} = k_{et} \exp(\beta E_a)$ = net frequency of electron transfer reaction.]

Note that this value is model independent as $f_{110}(k = 0)$ is related to the static dielectric constant ε_0. What is perhaps more interesting is the observation that the translational librational modes also contribute significantly to the Gaussian decay.

We have also discussed the effects of these ultra-fast modes on the electron-transfer dynamics in water and acetonitrile. Theoretical studies offer some interesting predictions, such as the energy diffusion control of the rate in acetonitrile. These predictions can be tested against experiments.

Acknowledgement

The work reported here was carried out in collaboration with my students, especially Ms Srabani Roy, Ms N. Gayathri and Dr N. Nandi. I thank Profs Graham Fleming, P. F. Barbara, M. Maroncelli, Iwao Ohmine, Masanori Tachiya and K. Yoshihara for sending me many of their preprints and also for valuable discussions. The work was supported by grants form the DST and CSI, India.

References

1. BAGCHI, B. — *A. Rev. Phys. Chem.*, 1989, **40**, 115–141.
2. BARBARA, P. F. AND JARZEBA, W. — *Adv. Photochem.*, 1990, **15**, 1–65.
3. MARONCELLI, M., MCINNIS, J. AND FLEMING, G. R. — *Science*, 1990, **243**, 1674–1683.
4. FLEMING, G. R. AND WOLYNES, P. G. — *Phys. Today*, 1990, **43**, 36–43.
5. BAGCHI, B. AND CHANDRA, A. — *Adv. Chem. Phys.*, 1991, **40**, 1–127.
6. MARONCELLI, M. — *J. Mol. Liq.* 1993, **57**, 1–37.
7. GAUDUEL, Y. — *J. Mol. Liq.*, 1995, **63**, 1–54.
8. ROSSKY, P. J. AND SIMON, J. D. — *Nature*, 1994, **370**, 263–269.
9. See the papers in *Ultrafast reaction dynamics and solvent effects* (Gauduel, Y. and Rossky, P. J., eds), 1994, AIP Press.
10. See the articles in *Ultrafast dynamics of chemical systems*, (Simon, J. D., ed.), 1994, Kluwer Academic.
11. JIMNEZ, R., FLEMING G. R., KUMAR, P. V. AND MARONCELLI, M. — *Nature*, 1994, **369**, 471–473.
12. FLEMING, G. R. — *Chemical applications of ultrafast spectroscopy*, 1986, Oxford University Press.
13. BAGCHI, B., FLEMING G. R. AND OXTOBY, D. W. — *Chem. Phys.*, 1984, **86**, 257–267.
14. ONSAGER, L. — *Can. J. Chem.*, 1977, **55**, 1819.
15. CALEF, D. F. AND WOLYNES, P. G. — *J. Chem. Phys.*, 1983, **78**, 470–482.
16. CHANDRA, A. AND BAGCHI, B. — *J. Chem. Phys.*, 1989, **91**, 2594–2598.
17. TACHIYA, M., — *Chem. Phys. Lett.*, 1993, **203**, 164–165.
18. ROY, S. AND BAGCHI, B. — *Chem. Phys.*, 1994, **183**, 207–216.

19. MARONCELLI, M. AND FLEMING, G. R. *J. Chem. Phys.*, 1988, **89**, 5044–5069.

*20. MARONCELLI, M., *J. Chem. Phys.*, 1991, **94**, 2084–2103.

21. ROSENTHAL, S. J., Xie, X., DU, M. AND FLEMING, G. R. *J. Chem. Phys.*, 1991, **95**, 4715–4717.

22. NERIA, N. AND NITZAN, A. *J. Chem. Phys.*, 1992, **96**, 5433–5439.

23. ROY, S. AND BAGCHI, B. *J. Chem. Phys.*, 1993, **99**, 1310–1319 and 9938–9943.

24. ROY, S., KOMATH, S. S. AND BAGCHI, B. *J. Chem. Phys.*, 1993, **99**, 3139–3142.

25. NANDI, N., ROY, S. AND BAGCHI, B. *J. Chem. Phys.*, 1995, **101**, 1390–1399.

26. ROY, S. AND BAGCHI, B. *Adv. Chem. Phys.*, 1995 (under preparation)

27. a. OHMINE, I. AND TANAKA, H. *J. Chem. Phys.*, 1990, **93**, 8138–8147.

b. OHMINE, I., TANAKA, H. AND WOLYNES, P. G. *J. Chem. Phys.*, 1988, **89**, 5852–5860.

c. STILLINGER, F. H. AND RAHMAN, A. *J. Chem. Phys.*, 1974, **60**, 1545–1557.

d. MADDEN, P. A. AND IMPEY, R. W. *Chem. Phys. Lett.*, 1986, **123**, 502–506.

28. RAINARI, F. O., RESAT, H. AND FRIEDMAN, H. L. *J. Chem. Phys.*, 1992, **96**, 3068–3084.

29. MARCUS, R. *A. Rev. Phys. Chem.*, 1964, **15**, 155–198.

30. ZUSMAN, L. D. *Chem. Phys.*, 1980, **49**, 295–304.

31. HYNES, J. T. *J. Chem. Phys.*, 1986, **90**, 3701–3709.

32. WEAVER, M. *Chem. Rev.*, 1992, **92**, 463–480.

33. BARBARA, P. F., *et al.* *J. Chem. Phys.*, 1992, **95**, 4188–4194; 1992, **96**, 7859–7862.

34. SMITH, B. B., STAIB, A. AND HYNES, J. T. *Chem. Phys.*, 1993, **176**, 521–537.

35. HYNES, J. T. *et al.* In *Perspectives in photosynthesis*, (J. Jortner and B. Pullman, eds), 1990, Kluwer.

36. ROY, S. AND BAGCHI, B. *J. Phys. Chem.*, 1994, **98**, 9207–9215.

37. ROY, S. AND BAGCHI, B. *J. Chem. Phys.*, 1995, **102**, 7937–7944.

38. ROY, S. AND BAGCHI, B. *J. Chem. Phys.*, 1995, **102**, 6719–6726.

39. RAINERI, F. O., ZHOU, Y., FRIEDMAN, H. L. AND STELL, G. *Chem. Phys.*, 1991, **152**, 201–220.

40. WEI, D. AND PATEY, G. N. *J. Chem. Phys.*, 1990, **93**, 1399–1411.

41. RAHMAN, A. AND STILLINGER, F. *J. Chem. Phys.*, 1974, **60**, 1545–1557.

42. GUILLOT, B. *J. Chem. Phys.*, 1991, **95**, 1543–1551.

43. MCMORROW, D. AND LOTSHAW, W. T. *J. Phys. Chem.*, 1991, **95**, 10395–10406.